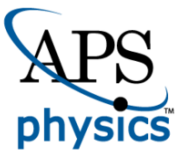

Bosonic Superfluid-Insulator Transition in Continuous Space

S. Pilati and M. Troyer

Phys. Rev. Lett. **108**, 155301 — Published 9 April 2012

DOI: 10.1103/PhysRevLett.108.155301

The bosonic superfluid-insulator transition in continuous space

S. Pilati
Theoretische Physik, ETH Zurich, 8093 Zurich, Switzerland and
The Abdus Salam International Centre for Theoretical Physics, 34014 Trieste, Italy

M. Troyer
Theoretische Physik, ETH Zurich, 8093 Zurich, Switzerland

We investigate the zero-temperature phase diagram of interacting Bose gases in the presence of a simple cubic optical lattice, going beyond the regime where the mapping to the single-band Bose-Hubbard model is reliable. Our computational approach is a new hybrid quantum Monte Carlo method which combines algorithms used to simulate homogeneous quantum fluids in continuous space with those used for discrete lattice models of strongly correlated systems. We determine the critical interaction strength and optical lattice intensity where the superfluid-to-insulator transition takes place, considering also the regime of shallow optical lattices and strong inter-atomic interactions. The implications of our findings for the super-solid state of matter are discussed.

PACS numbers: 67.85.Hj, 03.75.Hh

In quantum many-body systems, the interplay between inter-particle interactions and commensurability effects in external periodic potentials can induce a transition from a conducting (or superconducting) to an insulating phase, where particles are localized around the minima of the periodic potential. This phenomenon (known as Mott transition) is responsible for the insulating behavior of several transition metal compounds [1]. Recently, the Mott transition has been induced in a controlled way in both bosonic [2] and fermionic [3, 4] atomic gases trapped in optical lattices, which are being used as quantum emulators to explore the intriguing properties of strongly correlated materials [5].

Previous theoretical studies of cold atomic gases in optical lattices are based on single-band lattice models, such as the Bose- or Fermi-Hubbard models [6]. These theories are limited to the regime of large optical lattice intensity - since excited Bloch bands are neglected [6] - and weak interactions, since the true inter-atomic potential is replaced by a non-regularized δ-function, which corresponds to the first Born approximation for the scattering problem. The role of higher Bloch bands have been considered is Refs. 7, 8 (using the non-regularized pseudopotential), resulting in effective single-band models with density-dependent Hubbard parameters or many-body interactions. The description of interactions beyond the first Born approximation is a challenge, since more accurate pseudopotentials such as the regularized δ-function induce virtual transitions to an extremely large number of Bloch bands [9]. The validity of the single-band approximation has been questioned on a even more profound level by P. W. Anderson [10, 11], in particular concerning the existence of a bosonic Mott insulator. One central issue is the presence of nodes in the ground-state wave function of the bosonic Mott phase in the single band Hubbard model, since this is built on the basis of orthogonal - hence non-positive definite - Wannier functions. P. W. Anderson further argues that when all Bloch bands are included the superfluid component is always finite, implying that the solid phase is a supersolid.

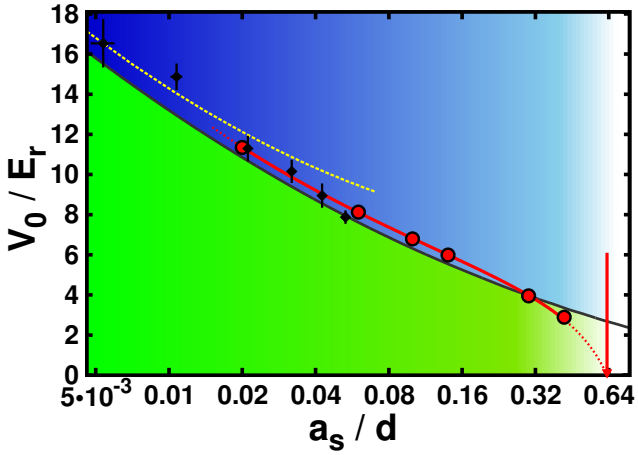

FIG. 1: (color online). Zero-temperature phase diagram as a function of the optical lattice intensity V_0/E_r and the s-wave scattering length a_s/d at unit filling. E_r is the recoil energy and d is the optical lattice periodicity. The red points indicate the transition from the superfluid (green region) to the insulating phase (blue region) for hard-sphere particles. The solid gray curve is the phase boundary of the single-band Bose-Hubbard model [28] (for a non-regularized δ-function interaction [6]). The dashed yellow curve is the multi-orbital model of Ref. [7] (obtained within mean-field approximation). The black diamonds are the experimental results of Ref. [12]. The solid red curve is a guide to the eye, the dashed red curve is an extrapolation towards the freezing point without optical lattice (red vertical arrow). See the text for other scenarios that are possible in this regime.

In this Letter we map out the zero-temperature and continuous-space phase diagram of a Bose gas with short-range interactions in a simple cubic optical lattice at a density of one particle per unit cell (see Fig. 1), using a new numerically exact hybrid quantum Monte Carlo

technique which permits to simulate the ground state of interacting Bose gases in arbitrarily weak or strong periodic potentials. Our main goal is to uncover the physics of the Mott transition in this continuous-space system, going beyond approximate discrete lattice models. We find a superfluid-to-insulator quantum phase transition, calculate the critical optical lattice intensity as a function of the s-wave scattering length, and compare our results to an experiment performed with an ultracold gas of Cs atoms [12], finding good agreement (see Fig. 1).

Bosons in an optical lattice are described by the continuous-space Hamiltonian

$$\hat{H} = -\frac{\hbar^2}{2m}\sum_{i=1}^{N}\left[\nabla_i^2 + V\left(\mathbf{r}_i\right)\right] + \sum_{i<j} v\left(\mathbf{r}_{ij}\right), \qquad (1)$$

where m is the atomic mass, the indexes i and j label the N particles at positions $\mathbf{r}_i$, and $\mathbf{r}_{ij} = \mathbf{r}_i - \mathbf{r}_j$. The optical lattice potential is $V\left(\mathbf{r}\right) = V_0 \sum_{\alpha=x,y,z} \sin^2\left(\pi\alpha/d\right)$, where V_0 is the intensity of the laser beams that create the lattice and d is half the wave-length.

The third term in Eq. (1) describes the two-body interactions. Different models for the inter-particle interactions can be considered, including potentials with a hard-core or with long-range interactions. One specific potential we use is the hard-sphere (HS) potential $v^{\mathrm{HS}}\left(r\right) = \infty$, if $r < a_{\mathrm{s}}$ and 0 otherwise. The diameter of the sphere is equal to the s-wave scattering length a_{s}, which is the parameter that characterizes the strength of interactions in dilute gases at low temperature. To quantify the role of other details of the inter-particle potential, which become relevant at high scattering energies and at short inter-particle distances, we also employ different models with the same s-wave scattering length, the negative-power potentials (NP) $v^{\mathrm{NP}}(r) = c/r^p$, with $c > 0$ and the integer $p > 3$ [13]. We do not consider attractive potentials supporting bound states, such as those used to model Feshbach resonances [14], since in this case the possible metastable gas-like phase is not the ground state.

To map out the phase diagram we employ a new algorithm combining the stochastic integration of variational trial wave-functions defined on a discrete lattice with an imaginary-time propagation in continuous space. The ground-state properties of a homogeneous quantum fluid ($V(\mathbf{r}) = 0$) can be obtained using the ground-state path-integral Monte Carlo method [15] (GSPI), where the expectation value of a generic operator $\hat{O}$ is obtained as

$$\langle\hat{O}\rangle = \frac{\int \mathrm{d}\mathbf{R}\mathrm{d}\mathbf{R}'\Psi_{\mathrm{T}}^*\left(\mathbf{R}\right)e^{-\frac{\beta}{2}\hat{H}}\hat{O}e^{-\frac{\beta}{2}\hat{H}}\Psi_{\mathrm{T}}\left(\mathbf{R}'\right)}{\int \mathrm{d}\mathbf{R}\mathrm{d}\mathbf{R}'\Psi_{\mathrm{T}}^*\left(\mathbf{R}\right)e^{-\beta\hat{H}}\Psi_{\mathrm{T}}\left(\mathbf{R}'\right)}, \qquad (2)$$

where $\mathbf{R} = \left(\mathbf{r}_1, \ldots, \mathbf{r}_N\right)$. For a sufficiently long imaginary time β, this expression gives the exact ground-state result provided that the trial wave function $\Psi_{\mathrm{T}}\left(\mathbf{R}\right)$ has a finite overlap with the ground state. The imaginary-time evolution operator $\exp\left(-\beta/2\hat{H}\right)$ can be represented in the form of a discretized path integral using the Trotter break-up, and the resulting multi-variates integral can be evaluated using standard Monte Carlo sampling techniques [16, 22]. However, the simulation of the strongly correlated regime in a periodic potential with the GSPI method is unfeasible with standard trial wave functions. We thus combine the GSPI algorithm with the stochastic sampling of variational wave-functions defined on a discrete lattice. The lattice wave function is characterized by the occupation numbers of a set of orbitals localized at the nodes of the lattice. Determining the expectation value (2) with such trial wave functions requires the sampling of those quantum numbers together with the continuous-space coordinates $\mathbf{R}$, as explained below.

As lattice wave function we use a bosonic Gutzwiller ansatz with contact interaction [17, 18] $\phi\left(\mathbf{l}_1, \ldots, \mathbf{l}_N\right) = \exp\left[-\gamma\sum_{i<j}\delta_{\mathbf{l}_i\mathbf{l}_j}\right]$, where $\delta_{\mathbf{l}_i\mathbf{l}_j}$ is the Kronecker delta, γ is a variational parameter and $\mathbf{l}$ refers to one of the sites of a simple cubic lattice. For the localized orbitals we consider a (positive definite) Gaussian approximation of the Wannier functions $w_{\mathbf{l}}(\mathbf{r}) = M^{-1/2}\sum_{\mathbf{k}}\exp\left(-i\mathbf{k}\cdot\mathbf{l}\right)b_{\mathbf{k}}(\mathbf{r})$, where M is the number of lattice sites and $b_{\mathbf{k}}\left(\mathbf{r}\right)$ is the Bloch function of the lowest band with quasi-momentum $\mathbf{k}$. For a given lattice configuration $\mathbf{L} = \left(\mathbf{l}_1, \ldots, \mathbf{l}_N\right)$, the coordinate-space wave function corresponding to $\phi\left(\mathbf{L}\right)$ is $\psi_{\mathbf{L}}\left(\mathbf{r}_1, \ldots, \mathbf{r}_N\right) = \prod_{i=1}^{N} w_{\mathbf{l}_i}\left(\mathbf{r}_i\right)$, so that the combined trial wave function is $\Psi_{\mathrm{T}}\left(\mathbf{R}\right) = \sum_{\mathbf{L}}\phi\left(\mathbf{L}\right)\psi_{\mathbf{L}}\left(\mathbf{R}\right)$, where the sum goes over all lattice configurations $\mathbf{L}$. To improve Ψ_{T} beyond the contact-interaction ansatz we introduce a Jastrow term $\chi\left(\mathbf{R}\right) = \prod_{i<j} f\left(\mathbf{r}_{ij}\right)$, giving a final trial wave function $\Psi_{\mathrm{T}}\left(\mathbf{R}\right) = \chi\left(\mathbf{R}\right)\sum_{\mathbf{L}}\phi\left(\mathbf{L}\right)\psi_{\mathbf{L}}\left(\mathbf{R}\right)$. The Jastrow correlation function [19] $f\left(\mathbf{r}\right)$ is set equal to the free-space solution of the two-body problem up to a cutoff distance r_{c}, and equal to 1 for $|\mathbf{r}| > r_{\mathrm{c}}$, as in Ref. 21. With this choice, the short-range correlations due to the hard-core of the inter-atomic interaction $v\left(\mathbf{r}\right)$ are treated exactly in the trial state Ψ_{T}, while the long-range correlations can be efficiently reproduced by the imaginary-time propagation. The time evolution also includes the effect of the higher Bloch bands.

To evaluate the right-hand side of Eq. (2) we need to perform a stochastic sampling over the lattice configurations $\sum_{\mathbf{L}}$ and the particle coordinates $\int \mathrm{d}\mathbf{R}$. This requires a random walk in the combined configuration space $\{\mathbf{L}, \mathbf{R}\}$, which we perform using local Monte Carlo updates on the lattice index $\mathbf{l}_i$ and the space coordinate $\mathbf{r}_i$ of a given particle i.

In the present problem, the bosonic statistics plays a central role. The trial state Ψ_{T} is by construction symmetric under particle exchange, and the imaginary-time propagation is symmetrized by performing particle permutations using the worm algorithm [22]. These permutations can efficiently introduce more exotic short-range correlations which are not explicitly included in the trial wave-function Ψ_{T} [23, 24].

For some specific values of γ the trial state Ψ_{T} reproduces wave-functions that have previously been used. When $\gamma \to 0$, Ψ_{T} converges to the "periodic+Jastrow"

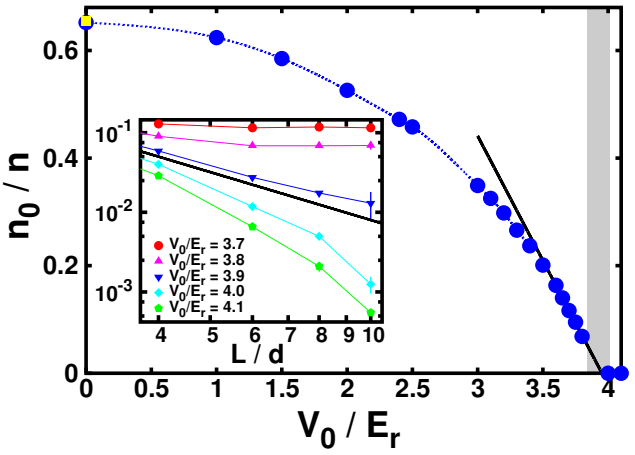

FIG. 2: (color online). Main panel: Condensate fraction vs. optical lattice intensity for HS with $a_s = 0.3d$ (blue bullets). The black solid line is a linear fit used to extract the critical point V_0^c. The yellow square at $V_0 = 0$ is the diffusion Monte Carlo result of Ref. [21]. Inset: finite-size scaling analysis of n_0, L is the simulation-box size. The black solid line is the scaling behavior expected at the critical point: $n_0 \propto L^{-2}$.

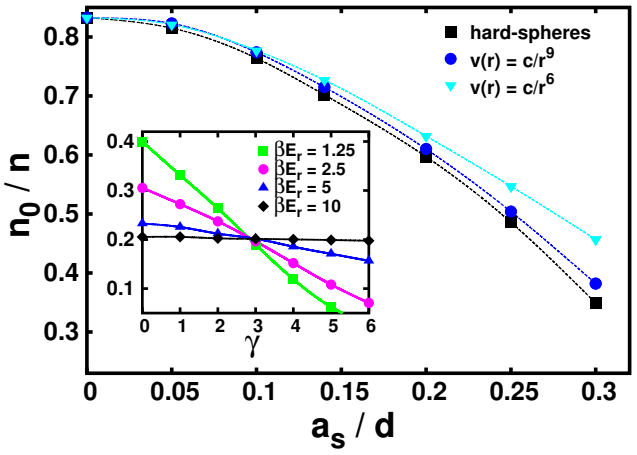

FIG. 3: (color online). Main panel: condensate fraction vs. s-wave scattering length a_s for different model potentials. The optical lattice intensity is $V_0 = 3E_r$. Inset: condensate fraction as a function of the variational parameter γ. Here $V_0 = 3.5E_r$ and $a_s = 0.3d$. The curves corresponding to different imaginary times β cross at the optimal γ.

wave-function $\Psi_T(\mathbf{R}) \simeq \chi(\mathbf{R}) \prod_i b_{\mathbf{k}=\mathbf{0}}(\mathbf{r}_i)$ [26] (ignoring an irrelevant normalization coefficient). This wave function accurately describes the ground state of a superfluid Bose gas in a periodic potential. In the opposite limit $\gamma \to \infty$ one obtains a symmetrized state with one particle per site [25] (we consider the case $N = M$) $\Psi_T(\mathbf{R}) \simeq \chi(\mathbf{R}) \sum_{\mathbf{P}(\mathbf{L})} \prod_i w_{\mathbf{p}(\mathbf{l}_i)}(\mathbf{r}_i)$, where the sum runs over the $N!$ permutations $\mathbf{P}(\mathbf{L}) = (\mathbf{p}(\mathbf{l}_1), \ldots, \mathbf{p}(\mathbf{l}_N))$ of N particles in $M = N$ lattice sites. In numerical studies of bulk Helium-4, a state analogous to this was introduced in order to describe a potential super-solid ground state [26, 27], where superfluidity coexists with diagonal long-range order (in this context it is referred to as "permanent+Jastrow", and the Wannier functions are replaced by effective localized orbitals). However, it has never been implemented in other exact quantum Monte Carlo methods such as the diffusion Monte Carlo because of the difficulty of performing random walks in permutation space. In the context of the single-band Bose-Hubbard model, the Gutzwiller ansatz $\phi(\mathbf{L})$ predicts, in the limit $\gamma \to \infty$, a quantum phase-transition from a superfluid to an insulating solid [17, 18]. This transition is also seen by exact lattice quantum Monte Carlo simulations [28]. Here we study this transition in the full Hilbert space of the continuum model, and investigate deviations from the single-band lattice model.

We identify the superfluid phase by measuring the condensate fraction [20], which is efficiently evaluated in the worm algorithm as $n_0/n = \lim_{|\mathbf{r}-\mathbf{r}'|\to\infty} \langle \hat{\Psi}^\dagger(\mathbf{r}') \hat{\Psi}(\mathbf{r}) \rangle$, where $\hat{\Psi}^\dagger$ ($\hat{\Psi}$) is the creation (annihilation) field operator. The results for the HS potential with $a_s = 0.3d$ are shown in Fig. 2. In the homogeneous limit $V_0 = 0$, we find agreement with the diffusion Monte Carlo prediction of Ref. 21 (yellow square). By increasing V_0, the condensate fraction decreases monotonically. Close to a critical optical lattice intensity (call it V_0^c), n_0 approaches zero linearly, consistently with the scaling law of the order-parameter in the Bose-Hubbard model $\langle \hat{\Psi}^\dagger(\mathbf{r}) \rangle = \sqrt{n_0/n} \approx \left[(V_0 - V_0^C)/V_0^C \right]^\beta$, where $\beta = 1/2$ (plus logarithmic correction) [29]. With a linear extrapolation to $n_0 = 0$ (black solid line in Fig. 2) we obtain the critical value $V_0^c/E_r = 3.95(10)$, where $E_r = \hbar^2\pi^2/2md^2$ is the recoil energy. Different extrapolation procedures yield compatible results. In order to better identify the quantum phase transition we perform a finite-size scaling analysis. In the inset of Fig. 2 we show n_0/n as a function of the simulation-box size L (we employ periodic boundary conditions) for different values of V_0. While slightly away from V_0^c the condensate fraction rapidly saturates to the thermodynamic limit, close to the critical point the scaling of n_0/n approaches the power-law $n_0 \propto L^{-2}$, which is indeed the scaling expected for the order parameter squared [29].

In the vicinity of the critical point V_0^c, the imaginary time β required to converge to the ground state scales with the size of the system. Hence, an accurate optimization of Ψ_T is important to avoid a possible bias due to the variational ansatz. Rather than by minimizing the ground-state energy, this optimization is achieved more conveniently with a finite imaginary-time scaling analysis, as shown in the inset of Fig. 3. The values of n_0/n obtained with a small imaginary time β show a clear dependence on the variational parameter γ. This dependence vanishes for larger β. The crossing point of the curves of n_0/n vs. γ corresponding to different values of β provides the optimal value of γ which removes the

residual finite imaginary-time effects.

In the phase diagram of Fig. 1 we show V_0^c as a function of a_s. In the region $V_0 < V_0^c$ the condensate fraction is finite and the system is superfluid. The region where $n_0 = 0$ is instead identified as an insulating phase. The phase boundary obtained with the HS potential (red circles) is compared to that of the Bose-Hubbard model [28] (lower solid gray curve), based on the mapping to single-band models described in Ref. [6]. For $a_s \lesssim 0.3d$ and $V_0 \gtrsim 4E_r$, the two models follow the same trend, with small discrepancies due to the effect of higher Bloch bands, and to the different models for the inter-atomic potential (HS vs. non-regularized delta). The experimental data [12] (blak-diamonds) are consistent with both the continuum and lattice model, but are in better agreement with our continuum model. The yellow dashed curve in Fig. 1 corresponds to a Bose-Hubbard model with occupation-number dependent parameters due to multi-orbital effects, solved within mean-field approximation (from Ref. [7]), and clearly simulations going beyond mean-field will be important to compare this model to our continuum results.

In the regime $a_s \gtrsim 0.3d$ the HS result bends down, as one approaches the freezing density of hard-spheres in free space $V(\mathbf{r}) = 0$ [30] (red vertical arrow). This region of the phase diagram could host more exotic phases, like a quantum-glassy phase eventually coexisting with superfluidity, due to the competition between the spatial symmetry of the optical lattice (simple cubic) and that of the hard-spheres crystal in free space (face-centered cubic). We leave the investigation of these issues to future work.

In this part of the phase diagram universality in terms of a_s is lost and also other details of the inter-atomic potential become important. We quantify these non-universal effects in Fig. 3 (main panel) by comparing the results for n_0/n vs. a_s/d (at fixed $V_0 = 3E_r$) obtained with different model potentials. The data corresponding to HS (black squares) and to NP with $n = 9$ (blues circles) agree within 10% up to $a_s = 0.3d$, indicating a large degree of universality. As expected, the data for NP with $n = 6$ (cyan triangle) show larger deviations. Notice that for $n < 6$ the effective range diverges [31]. In the limit $a_s \to 0$, n_0/n converges to $n_0/n = 0.833$, which is the square of the overlap between the condensate wavefunction (the Bloch state with $\mathbf{k} = \mathbf{0}$) and the plane wave with zero momentum.

Our results for the Mott transition in a continuous-space system of bosons with short-ranged interactions can be useful to extend experiments performed with ultracold gases to the regime of strong interactions and weak optical lattices, that is beyond the physics of the Hubbard model. While the existence of a quantum phase transition in the single-band model was rigorously proven [32], our findings indicate that quantum critical behavior persists when all Bloch bands are included, in contrast to the arguments of P. W. Anderson [10, 11].

The hybrid lattice-continuum quantum Monte Carlo method presented in this work can also be extended to fermionic models and be combined with fixed-node and transient-estimate techniques. This will provide a new approach for the simulation of strongly correlated fermionic systems in weak optical lattices.

We acknowledge J. Frölich and H.-P. Büchler for fruitful discussions, M. Mark and D.-S. Lühmann for providing their data. This work was supported by the Swiss National Science Foundation and a grant by the Army Research Office within the DARPA OLE program.

[1] N. F. Mott, *Metal-insulator transitions*, Taylor & Francis, London (1990).
[2] M. Greiner *et al.*, Nature **415**, 39-44 (2002).
[3] R. Jörderns *et al.*, Nature **455**, 204-207 (2008).
[4] U. Schneider *et al*, Science **322**, 1520 (2008).
[5] M. Lewenstein *e*t al., Adv. Phys. **56**, 243-379 (2007).
[6] D. Jaksch *et al*, Phys. Rev. Lett. **81**, 3108-3111 (1998).
[7] D.S. Luehmann, O. Juergensen and K. Sengstock, arXiv:1108.3013 (2011).
[8] U. Bissbort, F. Deuretzbacher, and W. Hofstetter, arXiv:1108.6047 (2011).
[9] H. P. Büchler, Phys. Rev. Lett **104**, 90402 (2010).
[10] P. W. Anderson, Science **324**, 631 (2009).
[11] P. W. Anderson, arXiv:1102.4797v1 (2011).
[12] M. J. Mark *et al.*, Phys. Rev. Lett. **107**, 175301 (2011).
[13] The scattering length of the NP potential is: $a_s = \left(\frac{2mc/\hbar^2}{(p-2)^2}\right)^{1/(p-2)} \frac{\Gamma[(p-3)/(p-2)]}{\Gamma[(p-1)/(p-2)]}$, where $\Gamma(x)$ is the Gamma function.
[14] C. Chin *et al.*, Rev. Mod. Phys. **82**, 1225 (2010).
[15] A. Sarsa *et al.*, J. Chem. Phys **113**, 1366 (2000).
[16] D. M. Ceperley, Rev. Mod. Phys. **67**, 279 (1995).
[17] D. S. Rokhsar and B. G. Kotliar, Phys. Rev. B **44**, 10328 (1991).
[18] W. Krauth, M. Caffarel and J. P. Bouchaud, Phys. Rev. B **45**, 3137 (1992).
[19] We impose continuity of $f(r)$ and of it's derivative in r_c.
[20] Strictly speaking, n_0/n is the occupation of the zero momentum state. One has $n_0 \neq 0 \Leftrightarrow n_c \neq 0$, where n_c is the occupation of the Bose-Einstein consensate.
[21] S. Giorgini, J. Boronat and J. Casulleras, Phys. Rev. A **60**, 5129 (1999).
[22] M. Boninsegni, N. V. Prokof'ev and B. V. Svistunov, Phys. Rev. E **74**, 036701 (2006).
[23] T. A. Kaplan, P. Horsch and P. Fulde, Phys. Rev. Lett. **49**, 889 (1982).
[24] M. Capello *et al*, Phys. Rev. Lett. **99**, 056402 (2007).
[25] The case $\gamma = \infty$ is simulated with a fictitious finite γ, measuring observables only when $\mathbf{l}_i \neq \mathbf{l}_j$ for $j \neq i$.
[26] D. Ceperley, G. V. Chester and M. H. Kalos, Phys. Rev. B **17**, 1070-1081 (1978).
[27] C. Cazorla *et al.*, New J. Phys. **11**, 013047 (2009).

[28] B. Capogrosso-Sansone, N. V. Prokof'ev and B. V. Svistunov, Phys. Rev. B **75**, 134302 (2007).
[29] M. P. A. Fisher *et al.*, Phys. Rev. B **40**, 546 (1989).
[30] M. H. Kalos, D. Levesque and L. Verlet, Phys. Rev. A **9**, 2178 (1974).
[31] N. F. Mott and H. S. W Massey, *The theory of atomic collisions*, Oxford University Press (1965).
[32] R. Fernandez, J. Fröhlich and D. Ueltschi, Commun. Math. Phys. **266**, 777-795 (2006).